Diurnal cycle of the Intertropical Convergence Zone in the east Pacific

C. L. Bain,[1,2] G. Magnusdottir,[1] P. Smyth,[3] and H. Stern[4]

Received 27 July 2010; revised 15 September 2010; accepted 4 October 2010; published 4 December 2010.

[1] A data set of Intertropical Convergence Zone (ITCZ) extent and location in the eastern Pacific, 90°W–180°W, 0°N–25°N, is used to examine the diurnal cycle of cloudiness over the ocean. The data set was generated using a statistical model which utilizes 30 year, 3-hourly infrared (IR) satellite data from 1980 to 2009. The ITCZ envelope of convection has a significant diurnal cycle across the whole domain, and the area of cloudiness "pulses" in extent, peaking in the afternoon. The diurnal cycle of brightness temperatures within the ITCZ changes from east to west, but generally there are two minima in mean IR, implying cold cloud is at a peak: one in the morning, 0600–0900 LST, and another in the afternoon, 1300–1600 LST. Decomposition of cloud top temperatures show that high cloud is at a maximum in the early morning and midlevel cloud peaks in the afternoon. Low cloud is at a maximum in the late evening (2200–0000 LST) and is immediately followed by increases in high cloud, suggesting that the deepest convective systems grow rapidly, within a few hours overnight. There are seasonal changes in the diurnal cycle of cloud top temperature, and it is suggested that colder mean temperatures are more likely in the afternoon when the ITCZ is more extensive. This is shown via seasonal changes and also by comparing El Niño years, when ITCZ is more present, to La Niña years.

Citation: Bain, C. L., G. Magnusdottir, P. Smyth, and H. Stern (2010), Diurnal cycle of the Intertropical Convergence Zone in the east Pacific, *J. Geophys. Res.*, *115*, D23116, doi:10.1029/2010JD014835.

1. Introduction

[2] The Intertropical Convergence Zone (ITCZ) can be seen as an organized zonal band of convection in the central and eastern Pacific during boreal summertime (May to October), when large-scale low-level convergence and convection occurs north of the equator. Here we use a newly generated data set [*Bain et al.*, 2010] of ITCZ location and extent to characterize the diurnal cycle of convection within the ITCZ. The diurnal cycle has a strong signature in the tropics and presents an excellent framework, for example, for validating the cloud convection schemes that are used in global circulation models. The ITCZ data used in this study are available every 3 h, May through October, for 30 years from 1980 to 2009. The data set was created by a statistical model which identifies the ITCZ envelope of organized convection, rather than using a threshold of cold cloud. With this statistical approach, the ITCZ may include low clouds and clear sky if they are contained within the larger cloudy zone, and therefore represents the large-scale weather feature rather than deep convection only.

[3] Tropical precipitation is highly influenced by the diurnal cycle of insolation. Satellite and weather station observations have shown that the diurnal cycle has a greater influence over land than in oceanic regions [*Meisner and Arkin*, 1987; *Hendon and Woodberry*, 1993]. However, *Yang and Slingo* [2001] noted that the strong diurnal signal over land can have influence over adjacent ocean regions, up to several hundred kilometers. In the western Pacific, this behavior has been noted near to island territories [*Houze et al.*, 1981].

[4] The timing of convection is different for land and ocean, with deep convective peaks mostly in the late afternoon over land, and in the early morning over ocean [e.g., *Janowiak et al.*, 1994]. This was also found in the idealized modeling studies of *Liu and Moncrieff* [1997]. The early morning peak in convection is often followed by a second peak in cloud or rain in the afternoon. For example, *Chen and Houze* [1997] found that small cloud systems over the west Pacific Ocean had two peaks, one at 0300–0600 local standard time (LST), the other at 1500–1800 LST. Some studies refer to this second peak as being part of a semidiurnal cycle in convection over ocean. Not all observational studies have noted the second peak in convection, and there are varied opinions on the timing of the early morning peak.

[5] Table 1 summarizes some of the key observational studies on the diurnal cycle of convection over ocean regions. The papers have been highly summarized and the techniques often simplified to provide quick comparisons. It is recommended to consult individual papers for provision

[1]Department of Earth System Science, University of California, Irvine, California, USA.
[2]Now at Met Office, Exeter, UK.
[3]Department of Computer Science, University of California, Irvine, California, USA.
[4]Department of Statistics, University of California, Irvine, California, USA.

0148-0227/10/2010JD014835

Table 1. Summary of Leading Papers on Diurnal Cycle Observations Over the Ocean

Study	Region	Data	Record Time	Convective Peak Over Ocean
Gray and Jacobson [1977][a]	Tropics	surface station rainfall across tropics	12 years of 8 months (March–Oct 1961–1973)	Early morning peak (stronger if convection stronger), afternoon peak in tropical Atlantic
Dorman and Bourke [1979][a]	Pacific	ship rainfall observations	22 years (1950–1972)	Early morning peak
Wexler [1983]	ITCZ, Pacific and Atlantic	satellite IR threshold (240K)	1 month (Jul–Aug 1973) measurements at 1130 LST, 2330 LST	Early morning peak in majority of ocean region, afternoon peak in ITCZ
Augustine [1984]	W. Pacific (168°E–112°W)	satellite IR threshold (253K)	1 month (Aug 1979)	Afternoon peak with secondary morning peak
Albright et al. [1985]	W. Pacific and SPCZ	satellite IR threshold (255, 237, 218K)	2 months (Jan–Feb 1979)	Early morning peak in very deep clouds, afternoon peak in deep cloud
Meisner and Arkin [1987]	Pacific (175°E–25°E)	satellite IR threshold (235K)	3 years (1981–1984)	Afternoon peak in ITCZ, little cycle observed elsewhere
Fu et al. [1990]	Pacific (110°E–90°W)	satellite IR and VS threshold combined technique	2 months (Jul 1983, Jan 1984)	Early morning peak in deep cloud, which changes 20–40% in size; medium cloud peaks in afternoon which changes 10–20% in size
Hendon and Woodberry [1993]	Tropics	satellite IR threshold (230K)	1 year (1983–1984)	Early morning (0300–0900 LST)
Mapes and Houze [1993]	W. Pacific (80°E–160°W)	satellite IR threshold (198, 208, 235K)	3 years of 4 months (Nov 86 to Feb 87, Nov 87 to Jan 88, Nov 88 to Jan 89)	Early morning (also noted expansion of area in afternoon)
Janowiak et al. [1994]	Tropics	satellite IR threshold (215, 225, 235K)	4 years (1986–1990)	Early morning peak in cold cloud (0300–0600 LST), warmer cloud also present in afternoon
Nitta and Sekine [1994]	W. Pacific (140°E–160°W)	satellite IR threshold (250K)	10 years (1980–1990)	Early morning peak 0500–0800 LST and afternoon peak 1300–1500 LST in the ITCZ in summer
Chen and Houze [1997]	W. Pacific (80°E–160°W)	satellite IR threshold (208, 235, 260K) and buoy data	4 months (Nov 92 to Feb 93) TOGA COARE	Early morning peak in deep convection 0000–0600 LST. Smaller cloud systems peak in the afternoon, and the early morning
Dai [2001][a]	Global	rainfall from surface stations	22 years (1975–1997)	Early morning peak in rainfall (0000–0400 LST nonshowers, 0600 LST showers)
Yang and Slingo [2001]	Tropics	satellite IR threshold (230K) for deep convection	4 years winters and summers (1984/1985, 1986/1987, 1987/1988, 1991/1992)	Early morning (with afternoon peaks close to land)
Nesbitt and Zipser [2003][a]	Tropics	TRMM rainfall	3 years (1997–2000)	Early morning rainfall peak
Serra and McPhaden [2004][a]	Pacific (10°N–10°S)	Rainfall data from moored buoys	4 years (Jun 1997 to Dec 2001)	Early morning rainfall max (0400–0700 LST), afternoon max during Jul–Nov in N. Pacific and Dec–Mar in S. Pacific
Tian et al. [2004]	Tropics	satellite IR and UTH, removed clouds $T < 260K$	1 year (1999)	Early morning peak in deep convection (0600–1000 LST); afternoon convection peak in NW Pacific; UTH peaks at midnight
Yen [2005]	W. Pacific (90°E–170°W, 15°S–45°N)	satellite IR threshold (250K)	13 years (1980–1993)	Late morning and early afternoon
Kumar et al. [2006][a]	Indian Ocean	Triton buoy rainfall	2 years (2001–2003)	Early morning (0900 LST) and afternoon (1800–2100 LST) peaks in summer
Kikuchi and Wang [2008][a]	Global	TRMM rainfall	8 years (1998–2006)	Morning (0600–0900 LST) peak in rainfall; little seasonal variability over oceans
Yang and Smith [2008][a]	Global	TRMM rainfall	7 years (1998–2005)	Early morning (0000–0600 LST) is primary rainfall, afternoon secondary maximum (stratiform rain)
Yang et al. [2008][a]	Global	TRMM (TMI, PR) rainfall	7 years (1998–2005)	Early morning (0000–0600 LST) is primary rainfall, afternoon secondary maximum (stratiform rain)

[a]These papers are primarily concerned with the diurnal cycle of rainfall (the majority of papers look at the diurnal cycle of cloud).

of the full scope of results. Table 1 represents a selection of relevant papers; early papers (pre-1977) which mainly use surface station data have been excluded due to fewer observations. The studies shown are primarily derived from satellite data, ensuring coverage over remote ocean areas. The studies are mostly from the Pacific region; many additional studies from other ocean basins including the Atlantic are not shown.

[6] Table 1 demonstrates the range of differences between observational studies. In particular, many studies disagree on the timing of peaks in tropical cloud; these differences may be due to the analysis technique used, time of year and averaging. The results also vary depending on whether rain, cloudiness or cloud depth is analyzed. The majority of studies shown in the table relate to cloud. However, where rainfall is the primary interest, a footnote is given.

[7] All papers note the early morning maximum in cold cloud and rainfall excluding that of *Meisner and Arkin* [1987], who only found the afternoon peak in cold cloud in the ITCZ and South Pacific convergence zone (SPCZ) region and noticed little diurnal variability elsewhere. However, some papers note a single maximum in cloud or rainfall [e.g., *Dorman and Bourke*, 1979; *Meisner and Arkin*, 1987; *Dai*, 2001], whereas others show the presence of a second maximum or semidiurnal cycle [e.g., *Albright et al.*, 1985; *Yen*, 2005; *Yang et al.*, 2008]. Most recent papers have confirmed that there is a semidiurnal cycle, and this view appears to represent the current consensus.

[8] The reasons for disparities between studies becomes clearer in the detailed examination of the secondary maximum in rainfall by *Yang et al.* [2008] and *Yang and Smith* [2008]. Their papers demonstrate that the afternoon maximum in rainfall is likely the result of stratiform cloud and rain, which might not be sensed by thresholding techniques which look exclusively for cold cloud. This was noted previously by *Chen and Houze* [1997] as a possible reason for discrepancies among studies, i.e., why some of the studies did not find an afternoon peak in smaller cloud systems.

[9] Studies specifically relating to the ITCZ diurnal cycle of convection are less numerous. *Nitta and Sekine* [1994] presented the diurnal cycle over the west Pacific with emphasis on the ITCZ and SPCZ regions. They observed cold cloud in infrared (IR) satellite data, using a threshold of 250 K to determine deep convection. They noted that in the ITCZ region, the convection peaked in the early morning for most of the year, but there were two peaks in cloud during the summertime (0500–0800 LST and 1300–1500 LST) when the ITCZ region was more convectively active. *McGarry and Reed* [1978] discussed the ITCZ diurnal cycle in the Atlantic. The study was for boreal summertime only, during the most active period for African easterly waves. An afternoon maximum in convection was found, and the amplitude of the diurnal cycle was increased closer to the African coastline. They also found that the afternoon maximum in rainfall was primarily from cloud systems whose mass inflow encompassed large areas, implying that convergence and therefore uplift on the large scale was modulated to peak during afternoon hours. *Magnusdottir and Wang* [2008] found that the Atlantic ITCZ was mostly composed of isolated disturbances or African easterly waves, whereas the east Pacific ITCZ appeared more zonally elongated. Differences in the diurnal cycle of the two regimes may therefore be expected. Our study here will present results for the Pacific only.

[10] This paper aims to define the diurnal cycle of the ITCZ in the east Pacific. We have used our statistical model to detect the ITCZ in instantaneous satellite data. The advantage is that we are able to use the ITCZ labels to diagnose the reaction of the envelope of convection on short time scales (i.e., in 3-hourly data to investigate the diurnal cycle). The ITCZ is mostly only defined in the literature on long time-averaged time scales using cold cloud thresholding [e.g., *Waliser and Gautier*, 1993], meaning that this information has not been previously available for study of the diurnal dynamics of the ITCZ. The climatology of the ITCZ was described by *Bain et al.* [2010], along with an evaluation of the data set in comparison to thresholding techniques and human eye interpretation. Here, we address the short timescale diurnal variation of the ITCZ and also characterize its seasonal and longitudinal variability. Section 2 introduces the data set of ITCZ observations, section 3 describes the results and section 4 contains discussion and conclusions.

2. Data Set

[11] The data set of ITCZ location consists of a binary set of labels identifying presence/absence of ITCZ for each grid point in a 0.5 × 0.5 degree gridded IR satellite image. The IR data are provided by the GridSat database [*Knapp and Kossin*, 2007], and are from 90°W–180°W, 0°N–25°N on an evenly spaced grid. The ITCZ labels are available every 3 h, 1980 to 2009 from May through October. In the wintertime the ITCZ is less present, and weaker when it is present, and extratropical fronts intrude on the domain, making ITCZ identification more difficult.

[12] The labels are generated by a Markov random field statistical model, using IR data as input. The model calculates the probability of ITCZ presence at each grid point and classifies as ITCZ those points with probability greater than 0.5. This ensures that grid points which are more likely to be ITCZ then non-ITCZ are included in the ITCZ label. Results are not sensitive to the threshold of 0.5 because a large majority of grid points have probabilities of being ITCZ that are near to zero or one. The probabilities depend on the following factors: The likelihood (via Bayes rule) of the observed IR value at the grid point, the presence/absence of ITCZ at neighboring grid points in space and time, and the latitude location of the grid point. The dependence on neighboring grid points introduces a recursive aspect to the computation, and the location term ensures that only tropical features are identified as being part of the ITCZ. The technique of Gibbs sampling [*Geman and Geman*, 1984; *Gilks et al.*, 1996] is used to stochastically search for high-probability assignments of each grid point to ITCZ presence/absence, given the observed IR data. By this method, smooth, continuous regions of ITCZ are identified. Full details of the model and validation are given by *Bain et al.* [2010].

[13] *Bain et al.* [2010] found that this statistical method provided systematic improvement in labeling accuracy over other automated techniques when compared to human labelers. The statistical method was also more consistent with other automated techniques (i.e., thresholding of IR and total precipitable water) than they were with each other.

Effectively the model is able to emulate what a human would "see" as organized cloud belonging to the convergence zone as opposed to isolated convection. This method of identification finds the ITCZ envelope of convection and is therefore useful for assessing diurnal changes in internal ITCZ characteristics as well as the large-scale structure.

[14] Figure 1a shows the study domain highlighted by a black rectangle. The ITCZ labels are split into different time zones so that the results can be corrected for local time (LST), these are indicated by black and gray dashed lines. The black dashed lines in Figure 1a split the domain into three boxes. These boxes are used in Figure 4 to study differences in the characteristics of the diurnal cycle from east to west. Figure 1b is an example of an ITCZ label objectively identified by the statistical model. The ITCZ label encloses the main region of convection but does not include small disturbances which are isolated from the large-scale structure. Figure 1c shows the same IR image with a threshold of 235K (as used by *Meisner and Arkin* [1987], *Mapes and Houze* [1993], *Janowiak et al.* [1994], and *Chen and Houze* [1997]) to contrast the methods used.

[15] The following analysis will make use of the absolute spatial extent of the ITCZ label, which will be used as a proxy for ITCZ area. In addition, we characterize the internal characteristics of the ITCZ by inspecting IR brightness temperatures within ITCZ labels.

3. Results and Analysis

3.1. Basic Diurnal Cycle of the ITCZ

[16] Figure 2 shows the diurnal cycle for ITCZ area and for mean IR temperature of the ITCZ labels. Figure 2 is an average from 1980 to 2009, from May to October. The plots have been corrected for LST for each longitude. *Bain et al.* [2010] show that the ITCZ was largest in area in the east Pacific, close to the Central American coastline. For this reason the anomaly from mean area was used in Figure 2a to allow comparisons between longitudes.

[17] Figure 2a demonstrates that despite the differences in mean area (not shown), the diurnal cycle in ITCZ area anomaly is very similar between longitudes. The ITCZ grows approximately 15% in size between 1400–2000 LST and shrinks up to 10% of its local size between 0000–1100 LST. In practice this means that the ITCZ envelope of convection "pulses" in accordance with the position of the Sun, and is largest after solar noon. It retracts its spatial extent during night hours. This pattern would lead to daily westward propagation of the amplitude of ITCZ area but not necessarily the individual cloud systems within the convective envelope. In instantaneous snapshots (such as in Figure 1), the ITCZ can sometimes be seen to be a relatively broken up feature. The analysis in Figure 2a is a mean over all days, even those when the ITCZ is not present. Therefore, the observed pulsing in area is true for the individual parts of the feature when ITCZ is present, but this does not imply that if there is no ITCZ present in a particular region, that the region will necessarily become cloudy in the afternoon.

[18] Figure 2b shows the cycle in mean IR within the ITCZ envelope, where deeper clouds are associated with colder mean temperatures. Unlike the ITCZ area, there are some longitudinal differences in the diurnal cycle of IR. In the central Pacific region (150°W–180°W) there are two minima in mean IR, one in the early morning, 0600–0800 LST, and another in the afternoon, 1300–1500 LST. In the eastern Pacific (90°W–120°W), the minimum in brightness temperature is in the afternoon only (approximately 1500 LST). In the middle region (120°W–150°W), the cycle is less pronounced, the lowest minimum in temperature is in the afternoon, with a secondary, smaller minimum in the early morning. These differences in mean IR temperatures between the east and west of the domain are consistent with studies from other regions, indicating that proximity to land influences the timing of diurnal convection [*Yang and Slingo*, 2001]. Over land, mean IR is coldest in the late afternoon, which is consistent with the eastern part of our domain.

[19] To investigate the character of cloud within the diurnal cycle, the IR within the ITCZ was split into four temperature categories that approximately represent three different cloud types as well as clear sky. The values were chosen after inspecting the traits of different temperature intervals in a Hovmöller plot. Temperature intervals were selected which showed separate and distinct behavior to one another, as well as being roughly equivalent to different cloud types (i.e., approximate high, middle-level and low-level cloud temperatures).

[20] Figure 3 shows the diurnal cycle for these categories in the farthest west (165°W–180°W in black) and the region farthest east (90°W–105°W in gray) in the Pacific. The western region was chosen as it demonstrates the clearest semidiurnal cycle in low IR temperatures. The eastern region was chosen to highlight the different behavior in a region where the semidiurnal cycle is less obvious. Figure 3 shows that in the morning (0400–0800 LST), the low mean temperature is attributed to an increase in the coldest deepest cloud ($T < 220K$) at both longitudes. In the afternoon, the low mean temperature is attributed to a peak in midlevel cloud ($220K < T < 255K$), and a reduction in low-level warm cloud ($255K < T < 280K$), and clear sky/very low cloud ($T > 280K$). The increase in mean IR temperature in Figure 3a at 1000 LST in the black line (165°W–180°W) is due to the high cloud decreasing and the midlevel cloud growing but still close to a minimum. There is also a small increase in clear sky and low clouds at 1000 LST in the black lines (Figure 3b).

[21] Figure 3b demonstrates that the growth in very cold cloud systems (present at 0400 LST) happens rapidly between 0100–0400 LST. This is suggested because the increase in low-level cloud at 2200 LST is not followed by an increase in midlevel cloud, suggesting the clouds quickly change from low to high cloud.

[22] Figure 3 shows that similar patterns are evident in both the eastern and western data: the morning minimum in mean IR is due to an increase in high cloud and the afternoon minimum is due to an increase in midlevel clouds. The morning minimum is less pronounced in the eastern zone, 90°W–105°W (gray line), due to very small changes: there is more clear sky and low cloud, and slightly less midlevel cloud (approximately 3%). During the afternoon, the eastern zone shows a higher proportion of high cloud and less midlevel cloud. The resulting diurnal cycle has colder mean IR in the afternoon than the morning (in 90°W–105°W) due to a greater portion of clear sky/ low cloud in the morning, increasing the temperature in relation to the diurnal cycle, and a greater portion of high cloud in the afternoon.

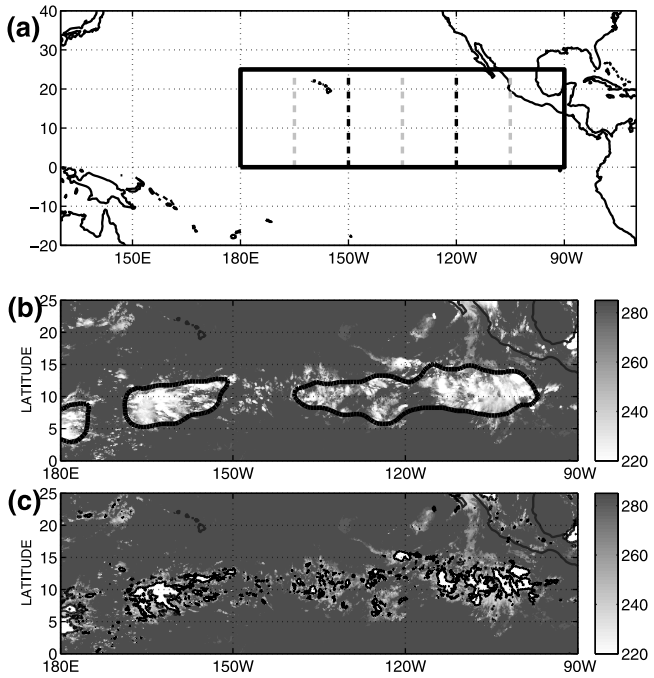

Figure 1. (a) Map of region, outlined in black. Longitudinal regions used for study indicated by black dashed lines; additional time zone splits indicated by gray dashed lines. (b) ITCZ label (black contour) identified by the statistical model and (c) ITCZ convection identified by IR threshold of 235K, overlaid on shaded IR satellite image on 17 August 2000 at 0000 UTC.

3.2. Seasonal Changes in the Diurnal Cycle

[23] To investigate seasonal changes in the diurnal cycle, the domain was split into three longitudinal regions and seasonal versus diurnal cycle diagrams of ITCZ area, and IR temperature within the ITCZ were examined. Results are shown in Figure 4. Seasonal changes in the diurnal cycle of brightness temperatures (Figures 4d–4f) are more apparent than the changes in the diurnal cycle of ITCZ area (Figures 4a–4c). Comparing across longitudes, the timing of the diurnal cycle in area (Figures 4a–4c) is similar between all longitude blocks: there is an increase in area anomaly from 1400–2000 LST, and area is at a minimum from 0000–1100 LST. However, the timing of the daytime minima in IR temperatures (Figures 4d–4f) differs from west to east and also across the season. Thus longitude differences in the diurnal cycle are more noticeable in IR than ITCZ area.

[24] Seasonal changes in the diurnal cycle of ITCZ area (Figures 4a–4c) are most notable in the east Pacific, 90°W–120°W, shown in Figure 4c, where diurnal variation is largest in July to mid-August. At this time, the ITCZ can pulse up to 40% of its mean size in the late afternoon (1800 LST), and contract by 20% in the morning (0900 LST). In the open ocean, at longitudes 150°W–180°W and 120°W–150°W (Figures 4a and 4b), seasonal changes are less distinct, but an increase in the anomalous growth of ITCZ in the afternoon is more apparent from July/August onward. Increases in anomalous growth occur at the same time in the season as increases in anomalous decline. This suggests that the magnitude of ITCZ pulsing in area is greater at certain points in the season.

[25] The IR diurnal cycle diagrams (Figures 4d–4f) show some significant seasonal and longitudinal variability in the diurnal cycle. The semidiurnal cycle in cold IR is seen with minima occurring at approximately 0700 LST and 1500 LST. The morning minimum is less distinct in the far east region (90°W–120°W, Figure 4f) but is present there from September onward. The strength of the minima in Figures 4d, 4e and 4f vary throughout the season. At times the minimum in temperature is more significant in the morning, whereas at other times the minimum is larger in the afternoon.

[26] Figures 4g, 4h, and 4i show the median area of ITCZ throughout the season. The seasonal changes in the timing of IR minima shown in Figures 4d, 4e and 4f correspond somewhat to seasonal changes in ITCZ occurrence, Figures 4g, 4h and 4i: Anomalously cold IR temperatures peak in the afternoon between 1200 and 1800 LST, more often at times when the ITCZ is larger in area. When the ITCZ is smaller, the coldest IR is in the morning hours, between 0600 and 0900 LST.

[27] In section 3.1 it was also discussed that in the eastern region where the ITCZ is larger, the afternoon IR temperatures are lower in relation to the diurnal cycle, and the IR minimum in the morning is less pronounced. To investigate if there was a relationship between afternoon IR and

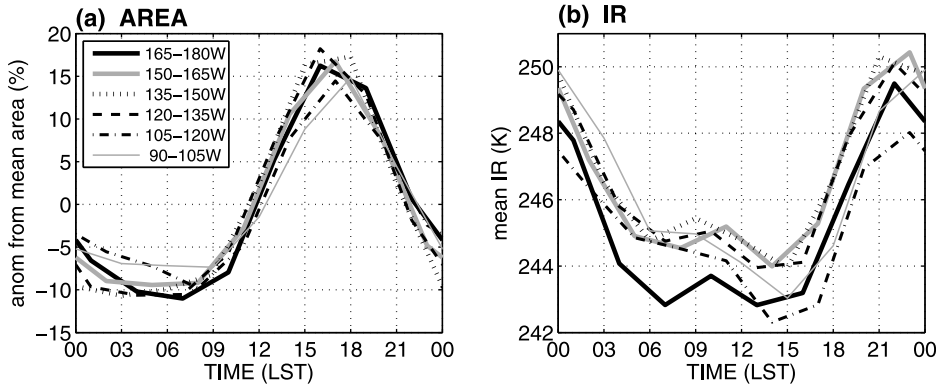

Figure 2. Diurnal cycle corrected for local solar time (LST) split into time zone longitudes. (a) Anomaly from mean area of ITCZ for each longitude (given as a percentage growth/decline). (b) Mean IR within ITCZ labels for each longitude (in K).

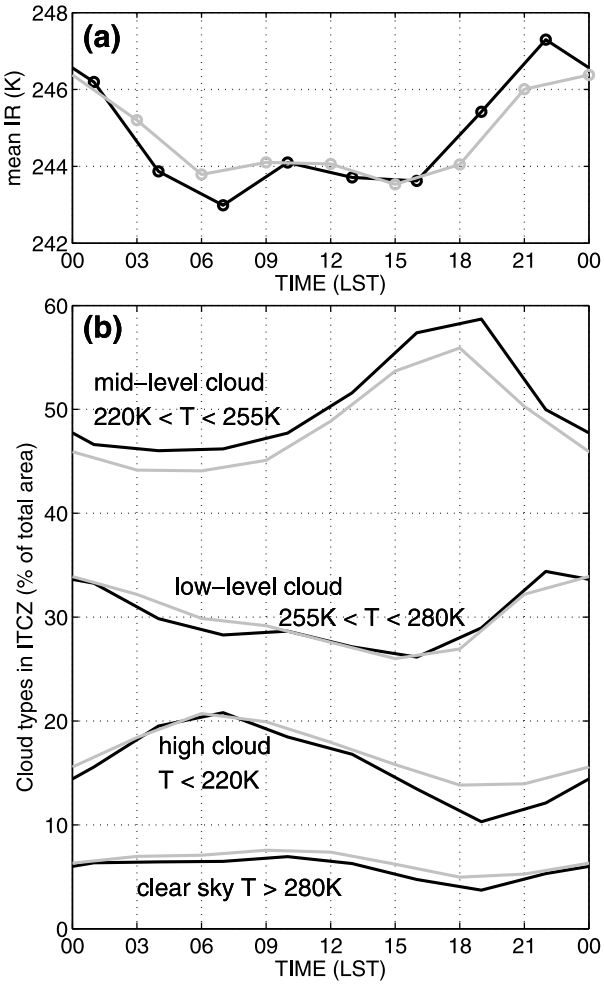

Figure 3. (a) Diurnal cycle of mean IR in ITCZ at 165°W–180°W (black contour) and 90°W–105°W (gray contour). (b) ITCZ (percent of total area) divided in three cloud categories and clear sky for each part of the diurnal cycle for 165°W–180°W (black contour) and 90°W–105°W (gray contour).

ITCZ area, the mean IR at 1500 LST was compared against ITCZ area for all longitude regions from 1980 to 2009. The seasonal cycle in temperature was removed by looking at anomalies from the daily mean IR rather than absolute values. Days when data were missing, or when the ITCZ was not present at the longitude tested could not be used due to lack of data, so the total number of days studied varied from west to east. The number of days used for each longitude is shown in Table 2. Figure 5 shows one example of the data from 120°W–135°W. A linear regression has been fit to the data. As is displayed, the data vary considerably from day to day around the line. A linear fit was applied to the same information for each longitude and the statistical results are displayed in Table 2.

[28] A negative, statistically significant (p value < 0.05) slope was found for longitudes 180°W to 135°W. The correlations are modest (ranging from −0.29 to −0.14) but the significance suggests that the finding is genuine. The low correlation values indicate that there are other factors which influence mean IR within the ITCZ. The relationships east of 135°W were not significant. The results suggest that in the open ocean, far from the Central American coastline, around 2–8% of the values of mean IR inside the ITCZ may be explained by changes in area of the ITCZ and this dependence is statistically significant. In contrast, close to the Central American coastline, the diurnal cycle in IR is independent of ITCZ area.

[29] The correlation between mean IR in the morning and area were also inspected (not shown). The correlations were smaller and less significant than the afternoon IR displayed in table 2. This may indicate that the clouds which characterize the morning ITCZ are independent of the size of the ITCZ.

3.3. Impact of ENSO on the Diurnal Cycle

[30] El Niño Southern Oscillation (ENSO) events have a significant impact on the character of the Pacific ITCZ. *Bain et al.* [2010] show that during El Niño years the ITCZ in the Pacific expands in size and frequency of occurrence, while during La Niña years the ITCZ is smaller and less present. Figure 6 is similar in format to Figure 2 but has been split into years where the ENSO index [*Wolter and Timlin*, 1998] is greater or less than 0.5 for three or more months during the summer.

[31] Despite changes in mean ITCZ area, Figures 6a and 6c show that the diurnal cycle in anomalies in ITCZ area is not noticeably impacted by ENSO. The only apparent change is in the far eastern longitudes, 90°W–105°W, where the diurnal cycle in area is marginally smaller in magnitude. In contrast, Figures 6b and 6d display more differences in IR signatures of the ITCZ between El Niño and La Niña years. During El Niño years, the mean IR temperatures within the ITCZ envelope are warmer. The ITCZ envelope of convection is larger during El Niño years, so a larger mean temperature may be attributed to clear sky or low cloud in between cold cloud systems; that is, the cloud is more broken up. The magnitude of the afternoon decrease in mean IR during El Niño years is similar to that during La Niña years, hence in relation to the rest of the cycle, the afternoon minimum is more significant during El Niño years.

[32] This is further explored in Figure 6e, where the IR cycle from La Niña years has been removed from the El Niño years to inspect the differences between them. There is variability between each longitude block which could be due to other dominating factors (e.g., land and coastline impacts) or the strength of local sea surface temperature changes. However, the mean (solid black line) of 180°W–105°W indicates that on average El Niño years have a colder mean IR in the late afternoon (approximately 1800 LST) than in La Niña years. This is not true for the longitudes east of 105°W, close to the Central American coastline. The comparison provided in Figure 6e may also indicate that IR was cooler in the morning (0300–0600 LST) during La Niña years, but again this is not true east of 105°W.

[33] To assess whether the pattern in Figure 6e reflects a real trend of a random pattern, the data were randomly divided into two groups of years and the difference from peak mean IR to low mean IR was computed. The deviation from zero of the solid line in Figure 6e had a p value of 0.09 when compared to lines obtained from the random data. This is borderline significance, but is only based on a data set of 11 El Niño years and 4 La Niña years. A more

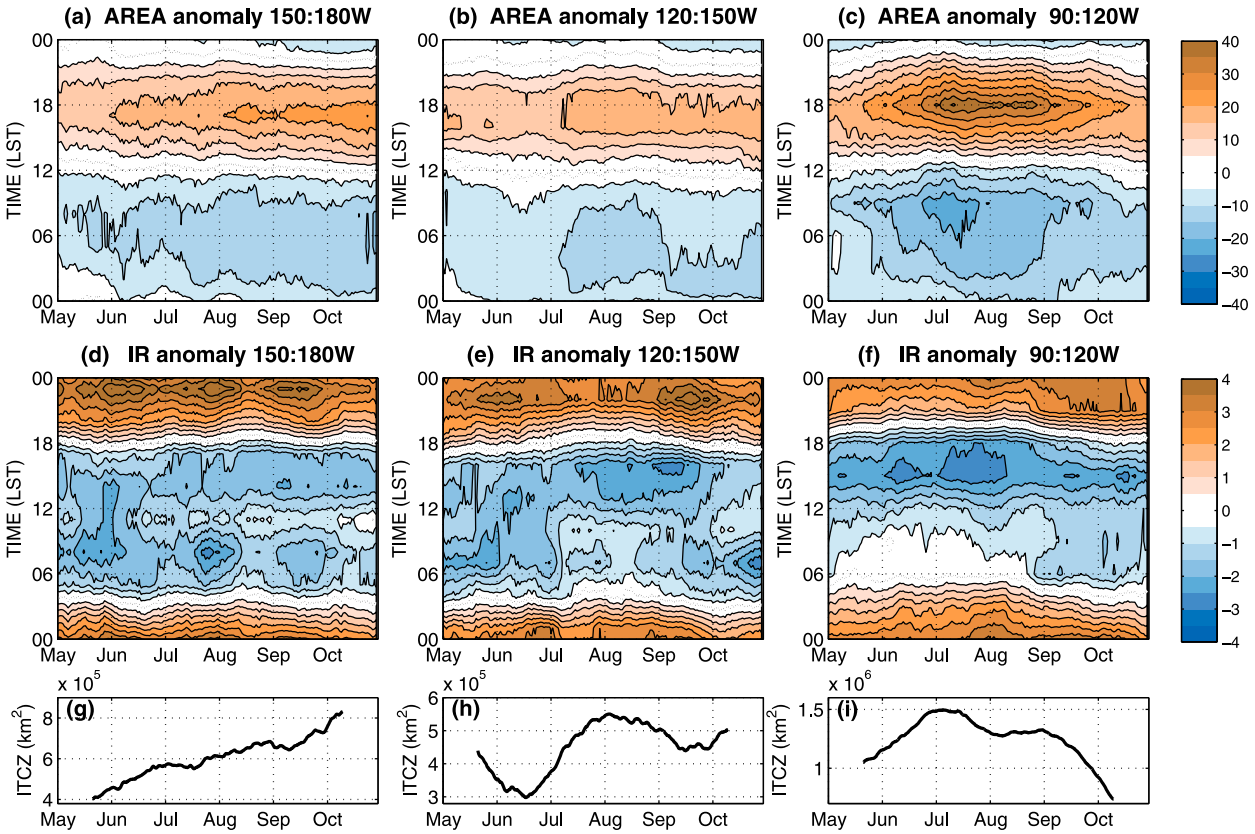

Figure 4. Diagrams showing the seasonal change in the diurnal cycle in: (a, b, c) anomalies in mean area of ITCZ going from west to east, as indicated by the black boxes in Figure 1a, and (d, e, f) anomalies in median IR of the ITCZ. The longitudes are identified above the plots. Figures 4a–4f have been smoothed with a 10 day running mean in the *x* direction. (g, h, i) The mean area of the ITCZ (1980–2009) for the plots in each column, smoothed with a 60 day running mean.

comprehensive analysis would require a much larger sample (e.g., 50 years), which is not currently available.

[34] Nonetheless, the results suggest that during El Niño years, mean IR temperatures within the ITCZ envelope of convection appear colder in the afternoon than in the morning, whereas during La Niña years a semidiurnal cycle of mean IR is more apparent. This result is not beyond the range of random variation, but a larger sample would be needed to investigate the behavior further.

4. Discussion and Conclusions

[35] It has been shown that the ITCZ in the east Pacific has a diurnal cycle in area and cloud top temperature. The area covered by the cloudy envelope "pulses" on a daily basis, where it grows on average 15% in size in the afternoon, and shrinks by 10% between 0000 and 0900 LST. This is the first study that we are aware of that presents this information on the ITCZ. The cycle in mean cloud top temperature is different in the east (90°W–120°W) from that in the central (150°W–180°W) Pacific. In the central Pacific, there are two minima in the mean brightness temperature of the ITCZ. One is in the early morning and one is in the afternoon. In the east Pacific, mean IR reaches a minimum in the afternoon. We observed that the afternoon minimum in mean IR appears to be at a lower temperature (in relation to the diurnal cycle) when the ITCZ is seasonally more present, and also during El Niño years in comparison to La Niña years.

[36] In section 3.1 it was shown that when the ITCZ is larger (in the eastern part of the domain), there is a small

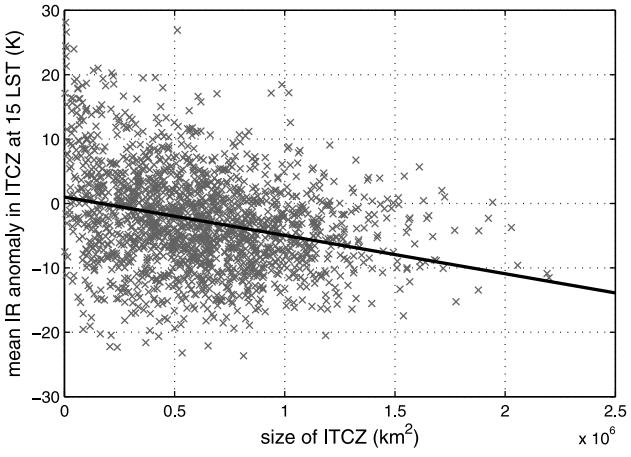

Figure 5. Relationship between size of ITCZ (km^2) and mean IR inside ITCZ label at 1500 LST for 135°W–150°W. There are 1793 days represented; statistical results of the fit are displayed in Table 2.

Table 2. Summary of Statistical Results From Comparing Area of ITCZ (km^2) and Mean IR Anomaly With Respect to the Diurnal Cycle (K) Within ITCZ at 1500 LST to Investigate Whether the Diurnal Cycle of Cloud is Impacted by the Size of the ITCZ

Longitudes	Number of Days	Gradient of Fit ($\times 10^{-6}$)	Standard Error	Correlation	p Value
165°W–180°W	1716	−0.25	0.35	−0.17	<0.001
150°W–165°W	1924	−0.52	0.39	−0.29	<0.001
135°W–150°W	1793	−0.60	0.49	−0.28	<0.001
120°W–135°W	2052	−0.23	0.37	−0.14	<0.001
105°W–120°W	3089	0.01	0.24	0.00	0.80
90°W–105°W	3086	−0.03	0.22	−0.03	0.14

increase in the proportion of low cloud (i.e., warmer temperatures) present in the early morning, while the proportion of medium-level cloud decreases slightly. The increase in warmer grid points may suggest that the distances between deep cloud during the early morning peak in convection is larger when the area of ITCZ is larger. This assertion is plausible because the alternative situation is unlikely: that the high clouds are as closely grouped together as in a small

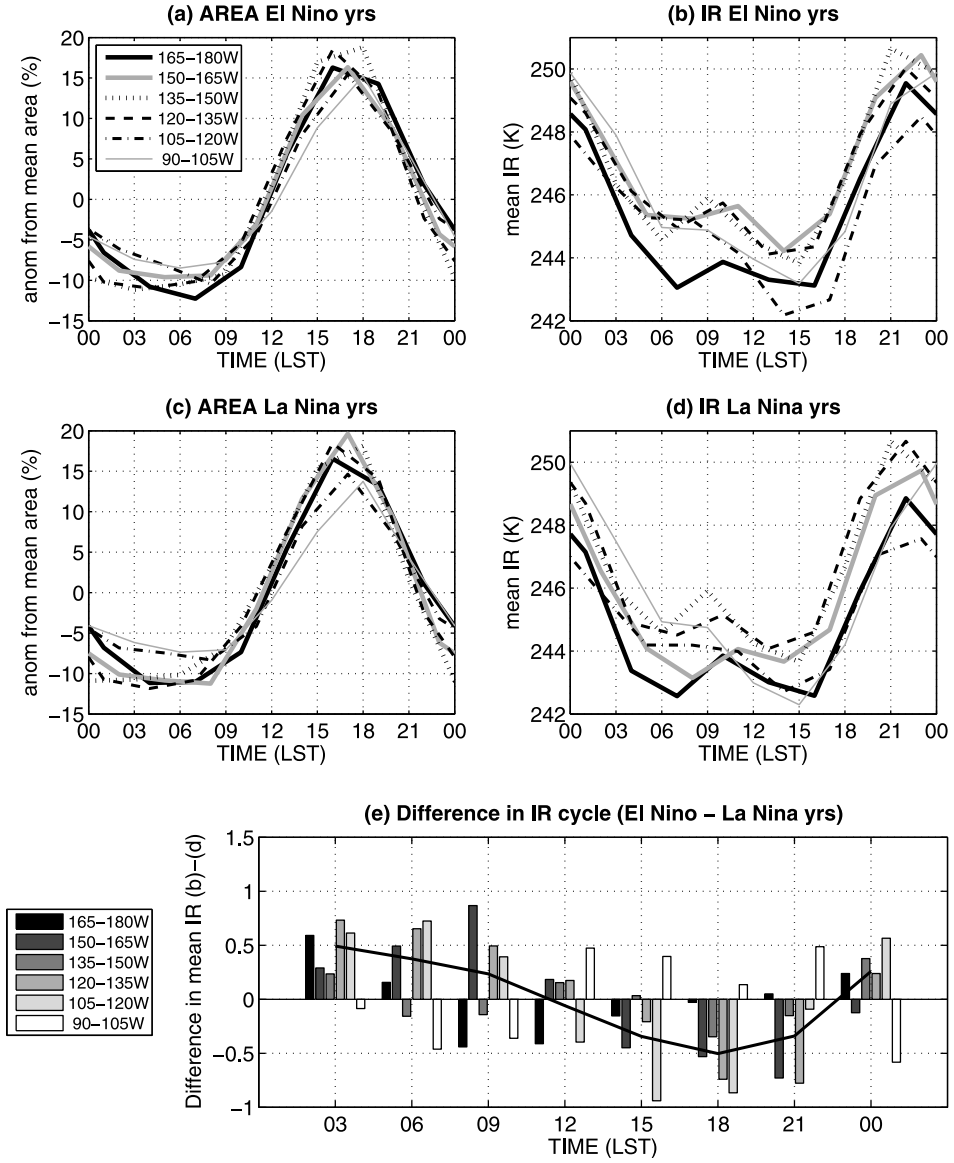

Figure 6. (a) Anomaly from mean area of ITCZ for El Niño years (1982, 1986, 1987, 1991, 1993, 1994, 1997, 2002, 2004, 2006, and 2009). (b) Mean IR within ITCZ labels for El Niño years. (c) Anomaly from mean area of ITCZ for La Niña years (1988, 1999, 2007, and 2008). (d) Mean IR within ITCZ labels for La Niña years. (e) Difference between Figures 6b and 6d in bars representing longitudes. The line is the mean from longitudes 180°W–105°W.

ITCZ, and low-level/clear sky is surrounding them, increasing the ITCZ area. This situation is unlikely because the statistical model uses probabilities based on IR value at a grid point and the surrounding grid points. Thus, if there were large regions on the edge of the ITCZ of warm cloud and clear sky without any cold cloud, it would not be labeled as ITCZ.

[37] Conversely, in the afternoon, the results indicate that a larger ITCZ implies a colder mean temperature in relation to the diurnal cycle. This might be simply because the earlier minimum in cold temperature is less pronounced and therefore the afternoon minimum is more distinct. Figure 3b also indicated that there was an increase in cold high cloud and a reduction in midlevel cloud during the afternoon minimum in the east compared to the west Pacific.

[38] Our findings suggest that there are several factors which may influence the timing of minimum temperature within the diurnal cycle. This may account for the variability in the timing of convective peaks among the studies identified in Table 1. In particular the following factors are likely to have influenced the findings of earlier studies.

[39] 1. The findings depend on how close to the continent the study is conducted: the closer to land, the more likely the mean IR reaches a minimum in the afternoon. The diurnal cycle of cloudiness is much stronger over land due to the larger diurnal cycle in surface fluxes. Land convection typically occurs in the late afternoon/evening, thus exerting influence over nearby ocean regions. Topography and coastline orientation may also have an impact on local ocean weather, influencing the timing of convection and rainfall. Figure 3 demonstrated that high cloud is more likely in the afternoon close to land than over open ocean, concurring with previous studies [*Yang and Slingo*, 2001].

[40] 2. The results are sensitive to the time span used for averaging, for example whether a study is at a particular time in the seasonal cycle or an annual average. We have shown that seasonal variations occur. This was also found by *Serra and McPhaden* [2004] but no seasonal variations were found by *Kikuchi and Wang* [2008]. It is possible that the signal was lost in the work by *Kikuchi and Wang* [2008] due to the dominating variability in the subtropics.

[41] 3. The findings depend on what the analysis techniques are identifying (is the study finding clouds or rain? total amount or intensity?). In particular, if thresholding is used, the timing of the diurnal peaks in cold cloud depends on the temperature being used for thresholding. Figure 3 showed the variability in convective peaks between high cloud ($T < 220K$) and midlevel cloud ($220K < T < 255K$). Indiscriminate thresholding of cold cloud is possibly not the best technique for characterizing the diurnal cycle over the ocean, due to different cycle timing depending on the level and type of cloud. In view of this, it is important to use alternative methods, such as our statistical model, to support the conclusions made from thresholding.

[42] To summarize, the primary results from this study are: (1) The area covered by the ITCZ envelope of convection pulses in size each day, reaching a peak in the late afternoon. (2) There are two daily minima in brightness temperature in the ITCZ over the open ocean. (3) The peak in deep, cold cloud in the morning suggests rapidly growing systems as it is not preceded by midlevel cloud. (4) The afternoon minimum in temperature appears more pronounced when the ITCZ is more extensive in area, during El Niño and during midsummer.

[43] This final point is consistent with findings by *Gray and Jacobson* [1977], *Meisner and Arkin* [1987], *Nitta and Sekine* [1994] and *Serra and McPhaden* [2004]. *Yang et al.* [2008] conjectured that the only plausible explanation for an afternoon maximum in convection is an "ocean surface heating" mechanism. However, this mechanism may not fully account for all situations when cold temperatures peak in the afternoon rather than the morning. The greater afternoon mean brightness temperature minimum is consistent with periods when the area covered by convection is greater, during El Niño years, and when the ITCZ is at a seasonal peak. These events do not obviously correspond to a large diurnal signature in SSTs. We therefore suggest that it is likely that changes in the strength of the afternoon peak in cold cloud is controlled by the atmospheric environment rather than surface conditions. The afternoon peak in cold cloud may also be greater at times when the morning peak in cold cloud is less pronounced due to decreased midlevel cloud and increased clear sky.

[44] **Acknowledgments.** The authors would like to acknowledge Jorge De Paz and Jason Kramer at UC Irvine for their work on the development of the statistical model. We would also like to thank Ken Knapp at NOAA's National Climatic Data Center for providing all IR data from the GridSat (HURSAT-Basin) archive. This research was supported by NSF grant ATM0530926 and NOAA grant NA09OAR4310132.

References

Albright, M. D., E. E. Recker, and R. J. Reed (1985), The diurnal variation of deep convection and inferred precipitation in the central tropical Pacific during January-February 1979, *Mon. Weather Rev.*, *113*, 1663–1680.

Augustine, J. A. (1984), The diurnal variation of large-scale inferred rainfall over the tropical Pacific ocean during August 1979, *Mon. Weather Rev.*, *112*, 1745–1751.

Bain, C. L., J. D. Paz, J. Kramer, G. Magnusdottir, P. Smyth, H. Stern, and C.-C. Wang (2010), Detecting the ITCZ in instantaneous satellite data using spatial-temporal statistical modeling: ITCZ climatology in the east Pacific, *J. Clim.*, doi:10.1175/2010JCL13716.1, in press.

Chen, S., and R. A. Houze (1997), Diurnal variation and life-cycle of deep convective systems over the tropical Pacific warm pool, *Q. J. R. Meteorol. Soc.*, *123*, 357–388.

Dai, A. (2001), Global precipitation and thunderstorm frequencies. Part II: Diurnal variations, *J. Clim.*, *14*, 1112–1128.

Dorman, C. E., and R. H. Bourke (1979), Precipitation over the Pacfic Ocean, 30°S to 60°N, *Mon. Weather Rev.*, *107*, 896–910.

Fu, R., A. D. Genio, and W. B. Rossow (1990), Behavior of deep convective clouds in the tropical Pacific deduced from ISCCP radiances, *J. Clim.*, *3*, 1129–1152.

Geman, S., and D. Geman (1984), Stochastic relaxation, Gibbs distribution and the Bayesian restoration of images, *IEEE Trans. Pattern Anal. Mach. Intell.*, *6*, 721–741.

Gilks, W., S. Richardson, and D. Spiegelhalter (1996), *Markov Chain Monte Carlo in Practice*, Chapman and Hall, Boca Raton, Fla.

Gray, W. M., and R. W. Jacobson (1977), Diurnal-variation of deep cumulus convection, *Mon. Weather Rev.*, *105*, 1171–1188.

Hendon, H. H., and K. Woodberry (1993), The diurnal cycle of tropical convection, *J. Geophys. Res.*, *98*, 16,623–16,637.

Houze, R. A., S. G. Geotis, F. D. Marks, and A. K. West (1981), Winter monsoon convection in the vicinity of north Borneo. Part I: Structure and time variation of the clouds and precipitation, *Mon. Weather Rev.*, *109*, 1595–1614.

Janowiak, J. E., P. Arkin, and M. Morrissey (1994), An examination of the diurnal cycle in oceanic tropical rainfall using satellite and in situ data, *Mon. Weather Rev.*, *122*, 2296–2311.

Kikuchi, K., and B. Wang (2008), Diurnal precipitation regimes in the global tropics, *J. Clim.*, *21*, 2680–2696.

Knapp, K. R., and J. P. Kossin (2007), New global tropical cyclone data from ISCCP B1 geostationary satellite observations, *J. Appl. Remote Sens.*, *1*, 013505, doi:10.1117/1.2712816.

Kumar, M. R. R., S. M. Pednekar, M. Katsumata, M. K. Antony, Y. Kuroda, and A. S. Unnikrishnan (2006), Seasonal variation of the diurnal cycle of rainfall in the eastern equatorial Indian Ocean, *Theor. Appl. Climatol.*, *85*, 117–122.

Liu, C., and M. W. Moncrieff (1997), A numerical study of the diurnal cycle of the tropical oceanic convection, *J. Atmos. Sci.*, *55*, 2329–2344.

Magnusdottir, G., and C.-C. Wang (2008), Intertropical convergence zones during the active season in daily data, *J. Atmos. Sci.*, *65*, 2861–2876.

Mapes, B. E., and R. A. Houze (1993), Cloud clusters and superclusters over the oceanic warm pool, *Mon. Weather Rev.*, *121*, 1398–1415.

McGarry, M. M., and R. J. Reed (1978), Diurnal variations in convective activity and precipitation during phases II and III of GATE, *Mon. Weather Rev.*, *106*, 101–113.

Meisner, B. N., and P. A. Arkin (1987), Spatial and annual variations in the diurnal cycle of large-scale tropical convective cloudiness and precipitation, *Mon. Weather Rev.*, *115*, 2009–2032.

Nesbitt, S. W., and E. J. Zipser (2003), The diurnal cycle of rainfall and convective intensity according to three years of TRMM measurements, *J. Clim.*, *16*, 1456–1475.

Nitta, T., and S. Sekine (1994), Diurnal variation of convective activity over the tropical western Pacfic, *J. Meteorol. Soc. Jpn.*, *72*, 627–641.

Serra, Y. L., and M. J. McPhaden (2004), In situ observations of diurnal variability in rainfall over the tropical Pacific and Atlantic oceans, *J. Clim.*, *17*, 3496–3509.

Tian, B., B. J. Soden, and X. Wu (2004), Diurnal cycle of convection, clouds, and water vapor in the tropical upper troposphere: Satellites versus a general circulation model, *J. Geophys. Res.*, *109*, D10101, doi:10.1029/2003JD004117.

Waliser, D. E., and C. Gautier (1993), A satellite-derved climatology of the ITCZ, *J. Clim.*, *6*, 2162–2174.

Wexler, R. (1983), Relative frequency and diurnal variation of high cold clouds in the tropical Atlantic and Pacific, *Mon. Weather Rev.*, *111*, 1300–1304.

Wolter, K., and M. S. Timlin (1998), Measuring the strength of ENSO events: How does 1997/98 rank?, *Weather*, *53*, 315–324.

Yang, G. Y., and J. Slingo (2001), The diurnal cycle in the tropics, *Mon. Weather Rev.*, *129*, 784–801.

Yang, S., and E. A. Smith (2008), Convective-stratiform precipitation variability at seasonal scale from 8 yr of TRMM observations: Implications for multiple modes of diurnal variability, *J. Clim.*, *21*, 4087–4114.

Yang, S., K.-S. Kuo, and E. A. Smith (2008), Persistent nature of secondary diurnal modes of precipitation over oceanic and continental regimes, *J. Clim.*, *21*, 4115–4131.

Yen, M.-C. (2005), Interannual variation of the diurnal convection cycle in the western North Pacific, *Meteorol. Atmos. Phys.*, *90*, 67–75.

C. L. Bain, Met Office, Exeter, EX1 3PB, UK.

G. Magnusdottir, Department of Earth System Science, University of California, Irvine, CA 92697, USA. (gudrun@uci.edu)

P. Smyth, Department of Computer Science, University of California, Irvine, CA 92697, USA.

H. Stern, Department of Statistics, University of California, Irvine, CA 92697, USA.